

FIRST-PRINCIPLES CALCULATIONS OF OXYGEN  
DIFFUSION IN Ti-Al ALLOYSS. E. Kulkova <sup>1,2</sup>, A. V. Bakulin <sup>1,2</sup>, S. S. Kulkov <sup>1</sup><sup>1</sup> National Research Tomsk State University,  
36 pr. Lenina, Tomsk 634050, RUSSIA<sup>2</sup> Institute of Strength Physics and Materials Science of  
the Russian Academy of Sciences, Siberian Branch,  
2/4 pr. Akademichesky, Tomsk 634055, RUSSIA  
e-mail: kulkova@ispms.ru

The projector augmented-wave method within the density functional theory is applied to investigate the oxygen diffusion in the intermetallic Ti-Al alloys. It is shown that the highest oxygen absorption energies in Ti-Al alloys correspond to the octahedral Ti-rich sites but the presence of aluminium in the nearest neighbours leads to a substantial decrease in the oxygen absorption energy in the alloys. The migration barriers for the oxygen diffusion between various interstices in the crystal lattice of the Ti-Al alloys are estimated. The preferred migration paths along *a* and *c* axes and limiting barriers of the oxygen diffusion in the alloys are determined. The dependence of the oxygen diffusion coefficient on Ti-Al alloy composition is discussed.

**Keywords:** *atomic diffusion, electronic structure, oxygen, Ti-Al alloys*

## 1. INTRODUCTION

Titanium aluminides are considered as the most promising structural materials for the aerospace and aviation applications due to their relatively low density, high melting point, high specific strength and modulus, good creep resistance, etc. [1], [2]. However, the oxidation resistance of Ti<sub>3</sub>Al and TiAl alloys is much lower than the desirable one that limits their application at high temperatures [1]–[5]. Although TiAl<sub>3</sub> alloy has the highest oxidation resistance among the Ti-Al alloys, it is a rather brittle material because of its low symmetry structure with few slip systems. It is known that the formation of a dense oxide film with a corundum  $\alpha$ -Al<sub>2</sub>O<sub>3</sub> structure on the surface of alloys with a low titanium content ensures their high oxidation resistance [6], [7]. However, the chemical activity of aluminium decreases with increasing titanium content that in combination with the thermodynamic characteristics of oxides implies a higher stability of interfaces with TiO and TiO<sub>2</sub> rather than

with  $\text{Al}_2\text{O}_3$  [8]. The growth of mixed oxide layers on the surface of the  $\text{Ti}_3\text{Al}$  and  $\text{TiAl}$  alloys is responsible for lower oxidation resistance. The outer layers of the oxide films, which are not in contact with the alloys, undergo cracking and partial spallation [9], [10]. Thus, the development of new high temperature structural materials based on titanium aluminides, the mechanical properties of which will be intermediate between the properties of nickel-based superalloys and high-temperature ceramics, is a challenging problem of modern materials science. Therefore, it is necessary to control the structure and properties of the surface layers of  $\text{Ti-Al}$  alloys and also the conditions of their oxidation. In this context, it is necessary to understand better the mechanism of surface oxidation of the  $\text{Ti-Al}$  alloys at the microscopic level. This implies theoretical studies of the interaction of oxygen with a surface and its diffusion from the surface into bulk and also in the bulk  $\text{Ti-Al}$  alloys in dependence on their composition. In the present research, we discuss the oxygen diffusion properties in the bulk of  $\text{Ti}_3\text{Al}$ ,  $\text{TiAl}$  and  $\text{TiAl}_3$  alloys.

## 2. METHOD OF CALCULATION

The calculations of atomic and electronic structure of binary alloys were performed by the projector augmented-wave (PAW) method [11], [12] within the density functional theory (DFT) implemented in the plane wave VASP code [13], [14]. The generalized gradient approximation (GGA-PBE) was used for the exchange-correlation functional [15]. The optimization of crystal structure was carried out whilst the forces at atoms were smaller than  $0.01 \text{ eV/\AA}$ . We used a full relaxation scheme, which included changes in the cell volume and its shape alongside with optimization of the atomic positions. A  $k$ -point mesh of  $7 \times 7 \times 7$  obtained according to the Monkhorst–Pack scheme was used for the integration over the Brillouin zone in the  $\text{TiAl}$  and  $\text{TiAl}_3$  bulk alloys. In the case of  $\text{Ti}_3\text{Al}$  alloy a  $\Gamma$ -centered  $k$ -point mesh of  $7 \times 7 \times 7$  was used. The oxygen absorption energy was calculated as follows:

$$E_{abs} = -[E_{\text{O/Ti-Al}} - E_{\text{Ti-Al}} - 1/2 E_{\text{O}_2}], \quad (1)$$

where  $E_{\text{O/Ti-Al}}$  and  $E_{\text{Ti-Al}}$  are the total energies of the bulk  $\text{Ti-Al}$  alloy with and without oxygen, respectively, and  $E_{\text{O}_2}$  is the total energy of the oxygen molecule. In order to calculate the oxygen atom migration barriers along possible paths, the Climbing Image Nudged Elastic Band method (CI-NEB) [16] was used. The initial positions of images along an elementary path were found by linear interpolation between the initial and final positions of a diffusing atom. During subsequent simultaneous relaxation of all images, each atom was assumed to be elastically bound to the same atom in the neighbouring images. Such an approach allows determining accurately a minimum energy path and a saddle point with the maximum energy. In this case, the relaxation of atomic positions was only performed. The height of the migration barrier was calculated as the difference in the total energies for system with the diffusing atom in the saddle point and in the initial one.

### 3. RESULTS AND DISCUSSION

The intermetallic  $\text{Ti}_3\text{Al}$ ,  $\text{TiAl}$  and  $\text{TiAl}_3$  alloys possess  $D0_{19}$ ,  $L1_0$  and  $D0_{22}$  structures, respectively, as shown in Fig. 1. The interstitial impurities such as oxygen, hydrogen, etc. prefer to be absorbed in the octahedral (O) or tetrahedral (T) interstices. All considered Ti-Al alloys are characterised by several types of the O- or T-sites having different compositions of Al and Ti atoms in the nearest environment. In case of  $\text{Ti}_3\text{Al}$  alloy, there are two O-sites: O1 at the centre of the octahedron formed by six Ti atoms, and O2 at the centre of the octahedron formed by four Ti atoms and two Al atoms. All tetrahedral sites in this alloy are formed by three Ti and one Al atoms. The latter atom can be located in the base of the tetrahedron (T1) or at its vertex (T2).

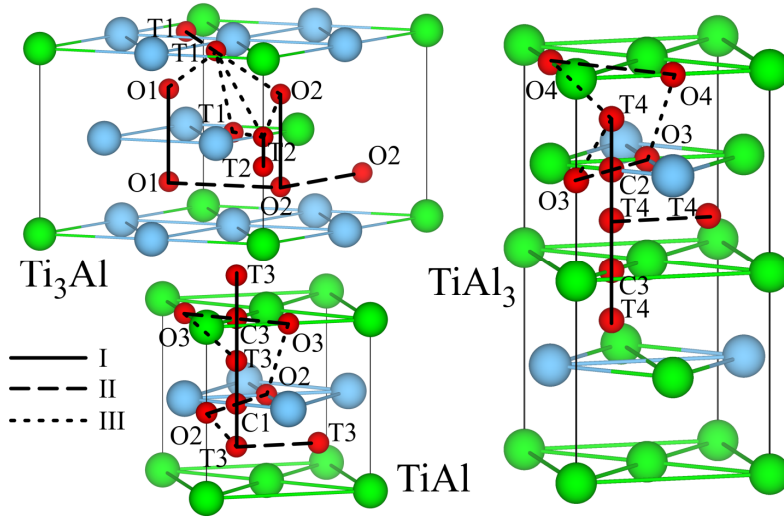


Fig. 1. Atomic structure and oxygen migration paths in the set of Ti-Al alloy. The positions between host atoms in the alloys, i.e., on Ti-Ti, Ti-Al and Al-Al bonds are marked by C1, C2 and C3, respectively.

On the contrary, in  $\text{TiAl}_3$  alloy the octahedrons are formed primarily by four or five Ti atoms and two or one Al atoms, respectively. The calculated absorption energies of oxygen are given in Table 1. It is seen that the Ti-rich sites are mostly preferable for the oxygen absorption in the bulk alloys that is in agreement with earlier calculations [17], [18]. In a number of works, e.g., [1], [19], it has been concluded that oxygen adsorption takes place on surface titanium atoms and the chemisorption rate decreases when the aluminum concentration in the alloy increases. Moreover, the kinetics for oxidation of Ti-Al alloys, especially at low temperatures, is mainly determined by the growth mechanisms of an oxide scale, i.e., diffusion, rather than surface processes. A slight energy preference of the Al-rich O4-site for the oxygen absorption in  $\text{TiAl}_3$  alloy is explained by the shift of oxygen towards the Ti atom and, as a result, by the smaller length of the Ti-O bond than in the O3-site, and also by the larger ionic contribution to the mechanism of chemical bond. The lower oxygen absorption energies at the tetrahedral sites correlate with the larger changes in the cell volume; i.e., oxygen can hardly be incorporated in these sites because of smaller

interstice volume. On the whole, the oxygen absorption energies in considered titanium aluminides decrease with an increase of Al atoms in the nearest neighbours and Al content in alloys (Table 1).

Table 1

The Oxygen Absorption Energies in Ti-Al Alloys

Alloys	O1 (6Ti)	O2 (4Ti+2Al)	O3 (2Ti+4Al)	O4 (1Ti+5Al)
Ti <sub>3</sub> Al	6.22	4.68	–	–
TiAl	–	4.02	3.07	–
TiAl <sub>3</sub>	–	–	2.76	2.91
Alloys	T1 (3Ti+1Al)	T2 (3Ti+1Al)	T3 (2Ti+2Al)	T4 (1Ti+3Al)
Ti <sub>3</sub> Al	4.58	3.77	–	–
TiAl	–	–	3.17	–
TiAl <sub>3</sub>	–	–	–	2.85

Let us discuss the diffusion of an oxygen atom along the paths shown in Fig. 1. All migration paths of an oxygen atom can be divided into three groups: (1) paths along the  $c$  axis, i.e., along [0001] or [001] directions in dependence on symmetry of Ti-Al alloy; (2) paths in the (0001) plane for Ti<sub>3</sub>Al or (001) one for TiAl and TiAl<sub>3</sub>; and (3) paths between sites in different (0001) planes in case of Ti<sub>3</sub>Al or (001) ones for other alloys but these sites are not one below another exactly. All calculated migration barriers are summarised in Fig. 2. In Ti<sub>3</sub>Al, the highest energy barrier for the oxygen diffusion was obtained between the Ti-rich O1-sites in the [0001] direction. It equals to 3.48 eV that is higher than that for the O2→O2 jump (3.02 eV) in the TiAl alloy. Note that both values for the migration barrier between the preferential O-sites are substantially higher than the value (2.05 eV) obtained for TiAl<sub>3</sub> [20]. Thus, despite the differences in the symmetry of the crystal lattices of the Ti–Al alloys, the energy barrier for the oxygen diffusion between the octahedral sites decreases with an increase of the Al content near an oxygen atom. Besides, in Ti<sub>3</sub>Al the migration barriers along the O1→O2 and O2→O2 paths in the basal (0001) plane are of ~0.5–0.9 eV lower than those for O1→O1 and O2→O2 along the  $c$  axis that can indicate the diffusion anisotropy in this alloy.

Although the migration barriers along the O2→O2 path in the [0001] direction and in the basal (0001) plane are lower than for the O1→O1 diffusion in Ti<sub>3</sub>Al, it takes higher energy for the O atom to be incorporated into the O2-site, which makes the diffusion between the O2-sites less preferred. In general, the oxygen migration between the T-sites is characterised by a low barrier; however, the path along the [0001] direction does not correspond to translation invariance and can be considered as part of the complex path, e.g., O2→T2→T2→O2. The energy barriers between the T-sites in the plane perpendicular to  $c$  axis are decreased in the set Ti<sub>3</sub>Al–TiAl–TiAl<sub>3</sub> (1.87–0.81–0.18 eV). It should be noted that in Ti<sub>3</sub>Al the energy barriers of the oxygen diffusion along the paths of the third type (O1→T1, O2→T1, O2→T2, etc., see Fig. 1) are higher than the corresponding barriers in TiAl and TiAl<sub>3</sub> alloys. Since the T-sites are less preferable for the O absorption, the reverse diffusion requires lower energy. Finally, it is shown that in TiAl the oxygen diffusion through the Al-layer is almost barrierless, while the migration barrier through the Ti-layer is significantly higher (2.17 eV).

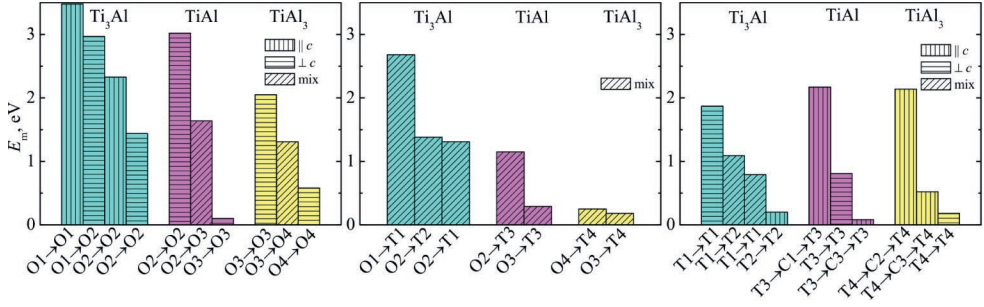


Fig. 2. The calculated migration barrier of oxygen in Ti<sub>3</sub>Al, TiAl and TiAl<sub>3</sub> alloys.

In contrast to [21], in our previous work [22] the diffusion coefficient  $D = D_0 \exp(-E_a/k_B T)$ , where  $D_0$  – the pre-exponential factor and  $E_a$  – the activation energy, was calculated using a specific value of frequency ( $\nu$ ) for each elementary jump and the corresponding energy barriers along the considered paths. A technique that is an extension of the theory proposed in [23] was used to describe the oxygen diffusion in  $\alpha$ -Ti. More details can be found in [22]. As is seen from Fig. 3a, the diffusion coefficient calculated using the energy barriers obtained within the DFT agrees well with the experimental data in [21]. The activation energies calculated from the diffusion coefficient of oxygen in the Ti<sub>3</sub>Al alloy along  $a$  and  $c$  axes are 1.99 and 1.97 eV, respectively, that agree well with the experimental data (1.94 and 1.92 eV, respectively [21]). The small diffusion anisotropy along two directions also agrees with the conclusion drawn from the experimental data in [21]. However, the oxygen diffusion in TiAl and TiAl<sub>3</sub> was not studied despite its importance in understanding the oxidation behaviour and the diffusion barrier properties of the Ti-Al alloys. It is seen from Fig. 3b that the diffusion coefficients of oxygen in both TiAl and TiAl<sub>3</sub> alloys are substantially higher than those in Ti<sub>3</sub>Al. The difference reaches five-seven order in case of TiAl and TiAl<sub>3</sub>. With an increase of the Al content, the anisotropy in the diffusion coefficients along  $a$  and  $c$  axes and also the oxygen diffusivity in the Al-rich alloys are increased. We remind that the oxidation resistance of the TiAl<sub>3</sub> alloy is caused by formation of the dense corundum oxide layers. The fast formation of this thin film prevents the interaction of oxygen with Ti atoms and formation of TiO<sub>2</sub> or mixed oxide scales. The established trends in absorption properties and migration barriers of O in the bulk alloys are valid for the O adsorption on surface and the O migration from the surface into the bulk.

Let us discuss the changes in a local electronic structure of the alloys during the oxygen diffusion along  $c$  axis. Figure 4 shows the total charge density distribution in the plane perpendicular to  $c$  axis and passing through the saddle points along different paths in Ti<sub>3</sub>Al and TiAl<sub>3</sub> alloys. In case of Ti<sub>3</sub>Al, the oxygen diffuses between two octahedral sites through the saddle point in triangle (Fig. 4a), whereas in TiAl<sub>3</sub> the saddle point is located in bridge position between two atoms (C2 or C3) and the end points are the tetrahedral sites (Fig. 4b). It is seen that in the saddle points the O–Ti bonds have ionic-covalent character, while the O–Al bonds are mainly ionic ones. The change of the charge density distributions has a local character and is accompanied by the shift of the nearest host atoms from O. Since the

covalent radius of Ti atom is larger by 0.14 Å than that of Al one, the presence of Al atoms as the nearest neighbours of oxygen in the saddle point results in an increase of the interstice volume. As a result, it is easier for O atom to be incorporated in this saddle point that leads to lowering of the migration barrier. It is seen in Fig. 4a that the interatomic distance between Ti and O atoms increases by 0.07 Å in presence of Al atom. On the other hand, the appearance of Al near oxygen leads to a decrease of the hybridization contribution that weakens the chemical bonds in saddle point as well. The similar picture can be seen in Fig. 4b.

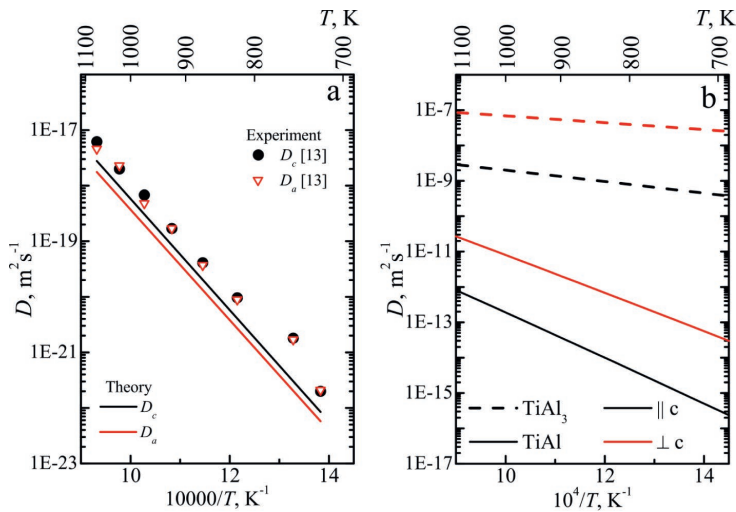


Fig. 3. The calculated diffusion coefficients of oxygen in (a) Ti<sub>3</sub>Al alloy in comparison with experimental ones and those (b) in TiAl and TiAl<sub>3</sub>.

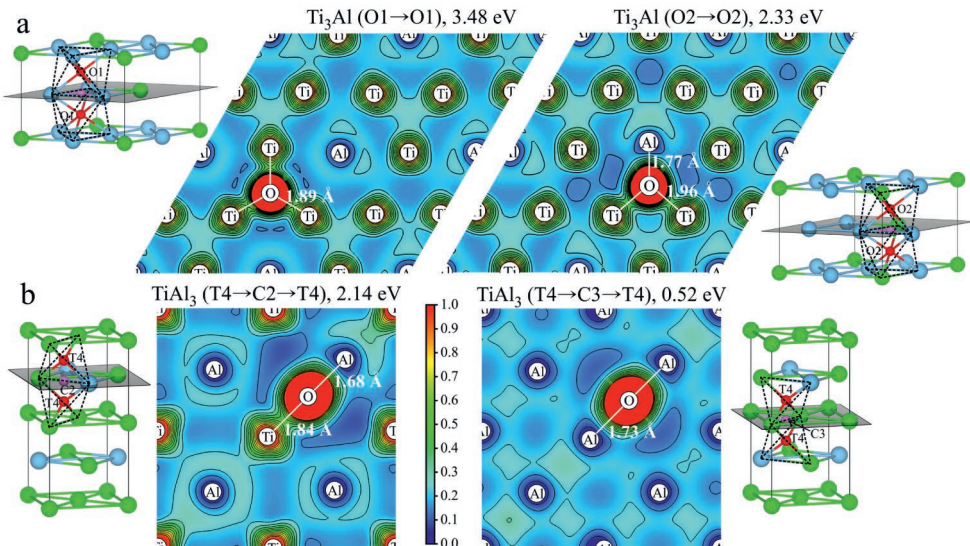


Fig. 4. Total charge density distribution in the plane passing through the oxygen and its nearest host atoms in saddle point for diffusion along c axis in Ti<sub>3</sub>Al (a) and TiAl<sub>3</sub> (b) alloys. The saddle and end points are shown in corresponding crystal structures.

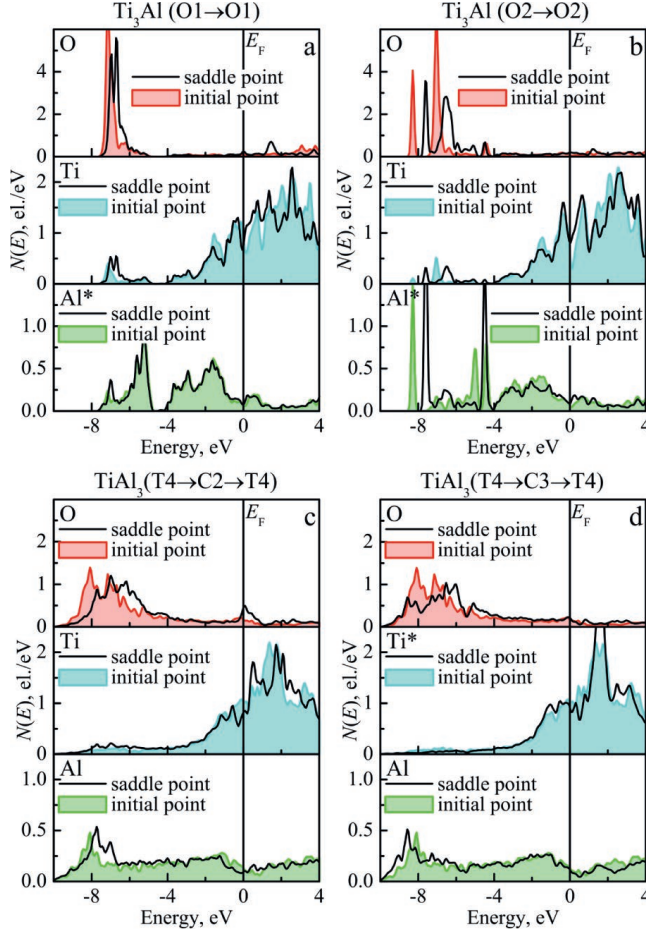


Fig. 5. Local DOS of oxygen and the nearest host atoms in initial and saddle points. The host atoms being the second nearest neighbors to oxygen are marked with symbol \*.

The comparison of the local densities of states of O and its nearest neighbour host atoms in the initial and saddle points is given in Fig. 5. It is seen that almost all DOS curves are shifted towards the Fermi level ( $E_F$ ) in the saddle points. In case of the O diffusion in  $Ti_3Al$  (Fig. 5a,b) the density of states at the Fermi level,  $N(E_F)$ , for Ti and Al atoms increases in the saddle points in comparison with the initial ones. Such changes in the electronic structure of the alloy can be considered as an indicator of structural instability. In the initial points the local DOSs and total ones, being not shown in Fig. 5a,b, have the local minimum in which  $E_F$  is located. The opposite effect is observed for the O diffusion between tetrahedral sites in the  $TiAl_3$  alloy (Fig. 5c). When O diffuses along the  $T4 \rightarrow C2 \rightarrow T4$  path, there is a decrease of  $N(E_F)$  especially in case of Ti atom, while an increase of  $N(E_F)$  occurs for O local DOS in the saddle point. However, the total DOS demonstrates the increase of  $N(E_F)$  in the C2 saddle point by 3.47 eL/eV. We remind that the tetrahedral site is less stable for oxygen in  $TiAl_3$  than the octahedral O4-site. For the O diffusion along the  $T4 \rightarrow C3 \rightarrow T4$  path, there are only small changes in the electronic structure of  $TiAl_3$  alloy in both initial and saddle points (Fig. 5d) that correlates with the low migration energy.

## 4. CONCLUSIONS

In the present research, the absorption and diffusion properties of oxygen in the Ti-Al alloys have been calculated by the PAW method within the DFT. It has been shown that the oxygen prefers mainly the Ti-rich octahedral sites in the bulk alloys. The appearance of aluminium in the nearest neighbours of oxygen leads to a decrease of its absorption energy in the set of  $\text{Ti}_3\text{Al-TiAl-TiAl}_3$  alloys. The greater solubility of oxygen in  $\text{Ti}_3\text{Al}$  is connected with existence of the octahedron formed by six Ti atoms. The energy barriers for the oxygen diffusion from preferred absorption sites decrease with an increase of aluminium content in the Ti-Al alloys. *Ab initio* estimations demonstrate that the diffusion coefficient and its anisotropy in the Ti-Al alloys increase also with the Al content. The Ti-rich sites can serve as oxygen traps, which retard the oxygen diffusion and hinder the aluminium oxidation. The obtained results can provide the better understanding of the oxygen diffusion properties in the Ti-Al alloys and the oxidation of intermetallic systems. Furthermore, such knowledge of the diffusivity and its anisotropy is very important in engineering and to predict the influence of impurities on the limiting diffusion barriers and the oxygen diffusion related properties. The effect of impurities on the oxygen diffusion rate in the Ti-Al alloys will be considered in our forthcoming paper.

## ACKNOWLEDGEMENTS

*The present research has partly been supported by the Russian Foundation for Basic Research under Grant 18-03-00064\_a, Institute of Strength Physics and Materials Science SB RAS (project III.23.2.8) and Tomsk State University Competitiveness Improvement Programme 2013–2020. Numerical calculations have been performed on the supercomputers at the National Research Tomsk State University and Lomonosov Moscow State University.*

## REFERENCES

1. Berdovsky, Y.N. (2008). *Intermetallics Research Progress*. New York: Nova Science.
2. Polmear, I. (2006). *Light Alloys: From Traditional Alloys to Nanocrystals*. Amsterdam: Butterworth-Heinemann.
3. Rahmel, A., & Spencer, P.J. (1991). Thermodynamic aspects of TiAl and  $\text{TiSi}_2$  oxidation: The Al-Ti-O and Si-Ti-O phase diagrams. *Oxid. Met.* 35(1/2), 53–68.
4. Kofstad, P. (1988). *High Temperature Corrosion*. London: Elsevier Applied Science.
5. Maurice, V., Despert, G., Zanna S., Josso, P., Bacos M.-P., & Marcus. P. (2007). XPS study of the initial stages of oxidation of  $\alpha_2\text{-Ti}_3\text{Al}$  and  $\gamma\text{-TiAl}$  intermetallic alloys. *Acta Mater.*, 55, 3315–3325. DOI: 10.1016/j.actamat.2007.01.030
6. Umakoshi, Y., Yamaguchi, M., Sakagami, T., & Yamane, T. (1989). Oxidation resistance of intermetallic compounds  $\text{Al}_3\text{Ti}$  and TiAl. *J. Mater. Sci.*, 24, 1599–1603.
7. Smialek, J.L., & Humphrey, D.L. (1992). Oxidation kinetics of cast  $\text{TiAl}_3$ . *Scripta Metall. Mater.*, 26, 1763–1768.
8. Okafor, I.C.I., & Reddy, R.G. (1999). The oxidation behavior of high-temperature aluminides. *JOM*, 51(6), 35–40.

9. Becker, S., Schutze, M., & Rahmel, A. (1993). Cyclic-oxidation behavior of TiAl and of TiAl alloys. *Oxid. Met.*, *39*(1/2), 93–106.
10. Wang, J., Kong, L., Li, T., & Hiong, T. (2016). High temperature oxidation behavior of Ti(Al,Si)<sub>3</sub> diffusion coating on  $\gamma$ -TiAl by cold spray. *Trans. Nonferrous Met. Soc. China*, *26*, 1155–1162. DOI: 10.1016/S1003-6326(16)64214-0
11. Blöchl, P.E. (1994). Projector augmented-wave method. *Phys. Rev. B.*, *50*(24), 17953–17979. DOI: 10.1103/PhysRevB.50.17953
12. Kresse, G., & Joubert, J. (1999). From ultrasoft pseudopotentials to the projector augmented-wave method. *Phys. Rev. B.*, *59*(3), 1758–1775. DOI: 10.1103/PhysRevB.59.1758
13. Kresse, G., & Hafner, J. (1993). *Ab initio* molecular dynamics for open-shell transition metals. *Phys. Rev. B.*, *48*, 13115–13118. DOI: 10.1103/PhysRevB.48.13115
14. Kresse, G., & Furthmüller, J. (1996). Efficiency of ab-initio total energy calculations for metals and semiconductors using a plane-wave basis set. *Comput. Mater. Sci.*, *6*, 15–50. DOI: 10.1016/0927-0256(96)00008-0
15. Perdew, J.P., Burke, K., & Ernzerhof, M. (1996). Generalized gradient approximation made simple. *Phys. Rev. Lett.*, *77*(18) 3865–3868. DOI: 10.1103/PhysRevLett.77.3865
16. Henkelman, G., Uberuaga, B.P., & Jónsson, H. (2000). A climbing image nudged elastic band method for finding saddle points and minimum energy paths. *J. Chem. Phys.*, *113*(22), 9901–9904. DOI: 10.1063/1.1329672
17. Wei, Y., Zhou, H.B., Zhang, Y., Lu, G.-H., & Xu, H. (2011). Effects of O in a binary-phase TiAl–Ti<sub>3</sub>Al alloy: From site occupancy to interfacial energetics. *J. Phys.: Condens. Matter.*, *23*(22), 225504. DOI: 10.1088/0953-8984/23/22/225504
18. Bakulin, A.V., Kulkova, S.E., Hu, Q.M., & Yang, R. (2015). Theoretical study of oxygen sorption and diffusion in the volume and on the surface of a  $\gamma$ -TiAl alloy. *J. Exp. Theor. Phys.*, *120*(2), 257–267. DOI: 10.1134/S1063776115020090
19. Shanabarger, M.R. (1998). Comparative study of the initial oxidation behavior of a series of titanium–aluminum alloys. *Appl. Surf. Sci.*, *134*(1–4), 179–186. DOI: 10.1016/S0169-4332(98)00196-2
20. Latyshev, A.M., Bakulin, A.V., Kulkova, S.E., Hu, Q.M., & Yang, R. (2016). Adsorption of oxygen on low-index surfaces of the TiAl<sub>3</sub> alloy. *J. Exp. Theor. Phys.*, *123*(6), 991–1007. DOI: 10.1134/S1063776116110133
21. Koizumi, Y., Kishimoto, M., Minamino, Y., & Nakajima, H. (2008). Oxygen diffusion in Ti<sub>3</sub>Al single crystals. *Philos. Mag.*, *88*(24), 2991–3010. DOI: 10.1080/14786430802419135
22. Bakulin, A.V., Latyshev, A.M., & Kulkova, S.E. (2017). Absorption and diffusion of oxygen in the Ti<sub>3</sub>Al alloy. *J. Exp. Theor. Phys.*, *125*(1), 138–147. DOI: 10.1134/S1063776117070019
23. Bertin, Y.A., Parisot, J., & Gacougnolle, J.L. (1980). Modèle atomique de diffusion de l'oxygène dans le titane  $\alpha^*$ . *J. Less-Common Met.*, *69*, 121–138.

# SKĀBEKĻA DIFŪZIJAS PIRMPRINCIPU APRĒĶINI Ti-Al SAKAUSĒJUMOS

S. E. Kulkova, A. V. Bakulins, S. S. Kulkovs

## K o p s a v i l k u m s

Projektora paplašinātā viļņa metode blīvuma funkcionālajā teorijā tiek izmantota, lai pētītu skābekļa difūziju intermetāliskajos Ti-Al sakausējumos. Rakstā parādīts, ka augstākās skābekļa absorbcijas enerģijas Ti-Al sakausējumos atbilst oktaedra Ti bagātām vietām, bet alumīnija klātbūtne tuvākajos reģionos ievērojami samazina skābekļa absorbcijas enerģiju sakausējumos. Tiek novērtētas migrācijas barjeras skābekļa difūzijai starp dažādām spraugām Ti-Al sakausējumu kristāla režģī. Pētījumā noteikti vēlami migrācijas ceļi gar a un c asīm un ierobežojošas skābekļa difūzijas barjeras sakausējumos. Tiek apskatīta skābekļa difūzijas koeficienta atkarība no Ti-Al sakausējuma sastāva.

12.11.2018.